Published in final edited form as:
J Immunol. 2009 November 15; 183(10): 6313–6319. doi:10.4049/jimmunol.0803422.

The mitochondrial uncoupling protein 2 (UCP2) inhibits mast cell activation and reduces histamine content †

Michael Tagen[1,+], **Alvaro Elorza**[2], **Duraisamy Kempuraj**[1], **William Boucher**[1], **Christopher L. Kepley**[3], **Orian S. Shirihai**[2], and **Theoharis C. Theoharides**[1,4,5]

[1] Molecular Immunopharmacology and Drug Discovery Laboratory, Department of Pharmacology and Experimental Therapeutics, Tufts University School of Medicine, Tufts Medical Center, Boston, MA 02111, USA

[2] Department of Medicine, Boston University School of Medicine, Boston, MA 02118, USA

[3] Luna Innovations Inc., Danville, VA 24541, USA

[4] Department of Biochemistry, Tufts University School of Medicine, Tufts Medical Center, Boston, MA 02111, USA

[5] Department of Internal Medicine, Tufts University School of Medicine, Tufts Medical Center, Boston, MA 02111, USA

Abstract

Mast cells are immune effector cells that are involved in allergies and inflammation through the release of mediators such as histamine, prostaglandins and cytokines. Uncoupling protein 2 (UCP2) is a mitochondrial protein that inhibits insulin secretion from β-cells, possibly through downregulation of reactive oxygen species (ROS) production. We hypothesized that UCP2 could also regulate mast cell activation. Here we show that mouse bone marrow mast cells (BMMCs) and human leukemic LAD2 mast cells express UCP2. BMMCs from *Ucp2*$^{-/-}$ mice exhibited greater histamine release, whereas overexpression of UCP2 in LAD2 cells reduced histamine release after both allergic and non-allergic triggers. *Ucp2*$^{-/-}$ BMMCs also had elevated histamine content and histidine decarboxylase expression. Histamine content was reduced by overexpression of UCP2 or treatment with the mitochondrial-targeted superoxide dismutase (SOD) mimetic TBAP. Furthermore, *Ucp2*$^{-/-}$ BMMCs also had greater production of both IL-6 and prostaglandin D_2 (PGD_2), as well as ERK phosphorylation, which is known to regulate prostaglandin synthesis. Intradermal administration of substance P (SP), an activator of skin mast cells, and challenge with DNP-HSA after passive sensitization induced significantly greater vascular permeability in the skin of *Ucp2*$^{-/-}$ mice *in vivo*. Our results suggest that UCP2 can regulate mast cell activation.

Keywords

UCP2; mast cells; histamine; IL-6; prostaglandins; mitochondria

Mast cells are critical mediators of allergic diseases, as well as innate and acquired immunity (1). Mast cells are found in areas exposed to the external environment and are

†This work was supported in part by the National Institutes of Health (2R01 AR047652 to T.C.T).

Address correspondence and reprint requests to: Theoharis C. Theoharides, Ph.D., M.D., Department of Pharmacology and Experimental Therapeutics, Tufts University School of Medicine, 136 Harrison Avenue, Boston, MA 02111, Phone: (617) 636-6866, Fax: (617) 636-2456, theoharis.theoharides@tufts.edu.
+Present Address: Department of Pharmaceutical Sciences, St. Jude Children's Research Hospital, Memphis, TN 38105, USA.

activated by diverse stimuli, including IgE receptor (FcεRI) crosslinking and neuropeptides such as substance P (SP) that act on G-protein coupled receptors (GPCRs). Mast cell granules store a number of preformed mediators, including histamine and proteases that are released by degranulation; activated mast cells also *de novo* synthesize numerous pro-inflammatory eicosanoids and cytokines many of which can be released selectively (2). These mediators cause immediate hypersensitivity reactions, characterized by vasodilation and increased vascular permeability, as well as late phase allergic inflammation (3). In spite of the increasing importance of mast cells in regulating immune processes (4), little is still known about how mast cell activation is regulated.

Uncoupling proteins (UCPs) reside on the inner mitochondrial membrane where they alter the mitochondrial membrane potential and reactive oxygen species (ROS) production (5). UCP2 in particular has been implicated in control of mitochondrial ROS production. Both mitochondrial and cytosolic ROS are produced by mast cell activation (6). Inhibition of ROS production reduces degranulation, indicating that ROS may play a role in regulating exocytosis (7,8). UCP2 activity inhibits exocytosis of insulin granules from pancreatic β-cells (9), and dopamine-containing vesicles from rat PC12 cells (10). UCP2 also dampens the inflammatory response of macrophages (11–13). We, therefore, hypothesized that UCP2 could inhibit mast cell activation and decrease mast cell-mediated inflammatory responses.

In this paper, we show that UCP2 is expressed in both murine and human mast cells. $Ucp2^{-/-}$ bone marrow-derived mast cells (BMMCs) have greater release of pro-inflammatory molecules after both allergic and non-allergic triggers, in addition to having increased histamine content. $Ucp2^{-/-}$ mice also develop significantly greater skin vascular permeability in response to SP and antigen after passive sensitization. Our results indicate UCP2 is a novel regulator of mast cell function with implications for treatment of mast cell-mediated allergic and inflammatory diseases.

Materials and Methods

Animals, isolation and culture of mast cells

$Ucp2^{-/-}$ and $Ucp2^{+/+}$ littermates were generated as previously described (11). Bone marrow cells were isolated from the femurs and tibias of age (8–12 weeks) and sex-matched mice. These cells were cultured in RPMI 1640 supplemented with 10% heat inactivated fetal bovine serum (FBS), 2 mM L-glutamine, 100 U/ml penicillin, 100 μg/ml streptomycin, non-essential amino acids, sodium pyruvate, 10 ng/ml murine stem cell factor (SCF) and 10 ng/ml murine IL-3 (both from Peprotech, Rocky Hill, NJ). Cells were used from 4–8 weeks of culture. Purity was tested by staining granules with toluidine blue (1%, pH 2). Fetal skin mast cells (FSMCs) were isolated and cultured as previously described (10). Cell suspensions were prepared from excised trunk skin of day 16 fetal mice by limited trypsinization. Cells were cultured for 3 weeks in media described above and purified by Percoll density gradient centrifugation prior to use in experiments. LAD2 cells (kindly supplied by Dr. A.S. Kirshenbaum, National Institutes of Health, Bethesda, MD) derived from a human mast cell leukemia (14) were cultured in StemPro-34 medium (Invitrogen) supplemented with 100 U/ml penicillin/streptomycin and 100 ng/ml rhSCF, kindly supplied by Amgen (Thousand Oaks, CA).

Skin histamine content

Age and sex-matched mice were sacrificed and an 8 mm diameter piece of dorsal skin was immediately removed and weighed. The skin was homogenized in 10 μl/mg of 2% perchloric acid and boiled for 10 min. After centrifugation at 10,000 *g* for 10 min, the supernatant was removed and neutralized with an equal volume of 2M NaOH. Histamine

levels were determined by commercial ELISA (Beckman Coulter, Fullerton, CA) according to the manufacturer's instructions.

Immunoblotting

Cells were washed once with PBS and then lysed in lysis buffer containing 20 mM Tris-HCl, pH 7.4, 1 mM EDTA, 150 mM NaCl, 1% NP-40, 1 mM PMSF, 10 μg/ml aprotinin, 10 μg/ml leupeptin, 1 mM Na_3VO_4, and 50 mM NaF. Equal amounts of protein were electrophoresed on 10% SDS-polyacrylamide gels (Invitrogen, Carlsbad, CA) and then transferred to a 0.44 μm PVDF membrane (Invitrogen). After blocking with 5% milk, membranes were probed overnight at 4°C with either goat anti-UCP2 (1:400, Santa Cruz) or rabbit anti-histidine decarboxylase (1:300, Abcam, Cambridge, MA). For detection, the membranes were incubated with the appropriate secondary antibody conjugated to HRP (1:5000, Santa Cruz) and the blots were visualized with enhanced chemiluminescence. Blots were then stripped and reprobed with antibodies against β-actin or porin.

c-Kit and FcεRI staining

BMMCs were sensitized with murine anti-DNP IgE (Sigma, St. Louis, MS) for the indicated period of time. The cells were resuspended in PBS and blocked with 5 μg/ml of FcγII/III blocking antibody (eBioscience, San Diego, CA) for 30 min at room temperature. After two washes, cells were incubated for 30 min at room temperature with either 5 μg/ml of FITC-conjugated anti-mouse IgE antibody, 1.25 μg/ml of PE-conjugated anti-mouse c-kit antibody, or the appropriate isotype control antibodies (all from eBioscience). Cells were then washed twice and analyzed with a FACSCalibur flow cytometer using CellQuest software (BD Biosciences, Lincoln Park, NJ).

RT-PCR and quantitative real-time PCR

RNA was isolated using the RNeasy mini-kit (Qiagen, Valencia, CA). RNA (500 ng) was reverse transcribed using the iScript cDNA synthesis kit (Ambion, Austin, TX). PCR reactions were performed using GoTaq Green Master Mix (Promega, Madison, WI) with the following cycling conditions: 95°C for 10 min and 35 cycles of: 95°C for 10 sec, 57°C for 60 sec. Products were run on a 2% agarose gel. The following primers were used: UCP2 F – 5′-TGTCTCGTCTTGCCGATTGAAGGT-3′; UCP2 R – 5′-TCTCGTGCAATGGTCTTGTAGGCT-3′; β-actin F – 5′-TGAGCGCAAGTACTCTGTGTGGAT-3′; β-actin R – 5′-TGTTTGCTCCAACCAACTGCTGTC-3′.

Quantitative PCR was performed in triplicate with an Applied Biosystems 7300 Real-Time PCR System using Taqman gene expression master mix (Applied Biosystems) and a Taqman murine histidine decarboxylase primer/probe set (Mm00456104_m1, Applied Biosystems,) and Taqman 18s rRNA primer/probe set (Applied Biosystems). Relative mRNA abundance was determined from standard curves run with each experiment and expression was normalized to 18s rRNA expression.

Histamine release assay

Mast cells were resuspended in Tyrode's buffer (137 mM NaCl,2.7 mM KCl, 20 mM HEPES, 5.6 mM glucose, 1.8 mM $CaCl_2$, 1.0 mM $MgCl_2$, and 0.1% bovine serum albumin, pH 7.4). Cells were stimulated either with SP (1 μM for LAD2 cells, 100 μM for BMMCs; Sigma), compound 48/80 (C48/80; 30 μg/ml) or ionomycin (1 μM; Sigma) for 10 min. BMMCs were sensitized overnight with anti-DNP IgE (100 ng/ml; Sigma) and stimulated with DNP-HSA (10 ng/ml; Sigma) for 20 min. LAD2 cells were sensitized overnight with human myeloma IgE (2 μg/ml; Chemicon, Billerica, MA) and stimulated with anti-human

IgE (10 μg/ml; Dako, Carpinteria, CA) for 20 min. Histamine levels in the supernatant and pellet were measured using a LS-50B Luminescence Spectrometer(PerkinElmer) as described (15) (41). Histamine release was expressedas percentage of the total cellular histamine content = (histaminein supernatant)/(histamine in supernatant + histamine in pellet) × 100.

IL-6 and prostaglandin D_2 assays

For IL-6 release, BMMCs (5×10^4 cells/500 μl) were distributed in 48-well microtiter assay plates and stimulated in complete culture medium with the indicated concentrations of stimulus for 24 hrs. IL-6 content was determined in cell-free supernatants with commercial ELISA kits (R&D Systems, Minneapolis, MN) according to the manufacturer's instructions. For prostaglandin production, BMMCs (2×10^5 cells/500 μl) were stimulated in Tyrode's buffer for 30 min. Commercial ELISAs for PGD_2 (PGD_2-MOX kit, Cayman Chemical, Ann Arbor, Michigan) were performed according to manufacturer's instructions.

ROS production

Cells were loaded with 5 μM dihydroethidium (Sigma) for 30 min at 37°C. The cells were washed twice, resuspended in Tyrode's buffer and stimulated as described. After 5 min of stimulation, cells were placed on ice until being analyzed using a FACSCalibur flow cytometer.

Lentiviral production and infection

Lentiviral vectors were generated as previously described (16). UCP2-encoding or pWPI vector with expression vectors encoding VSV-G gag-pol and env proteins were transiently transfected into 293T cells using Lipofectamine 2000 (Invitrogen). Supernatants were collected at 24 and 48 hours, filtered through 0.45 μm filters and centrifuged at 50,000×*g* for 2 hr at 4°C to pellet the virus. Viral pellets were resuspended in 300 μl culture media and frozen at −80°C until use. Cells were infected by spinoculation: 5×10^5 cells were resuspended in 200 μl fresh media and 50 μl viral suspension with 8 μg/ml polybrene (Sigma) in 12-well plates and spun at 1500×*g* for 90 min at 30°C. Afterwards, 1 ml of media was added and the next day the cells were resuspended in fresh media. Cells were used for experiments 5 days after infection.

Evans blue extravasation

Evan's blue (EB) extravasation was performed as previously described (17). Sex and age-matched mice were administered 1% EB in sterile normal saline (0.1 ml) via tail-vein injection. They were then anesthetized by an intraperitoneal injection (0.1 ml) of ketamine (100 mg/kg)/xylazine (10 mg/kg), following which the dorsal subscapular skin was shaved and either 50 pmol SP or 10 μg of histamine (both from Sigma, St. Louis, MO) were injected intradermally in a total volume of 50 μl in the subscapular region with a tuberculin syringe. After 20 min, mice were sacrificed and an 8 mm diameter circular piece of skin at each injection site was removed and weighed. Alternatively, we used passive cutaneous anaphylaxis: normal saline or anti-DNP IgE (20 μg/50 μl, Sigma) was administered intradermally at two skin sites each. Two days later, DNP-HSA (200 μg) along with 1% Evans blue in sterile normal saline (100 μl) was injected in the tail vein. The mice were sacrificed 30 min later, skin injection sites were cut, weighed and placed in Eppendorf tubes. The mice were then handled the same as described above. EB was extracted in 1 ml of N,N-dimethylformamide overnight at 55 °C and the optical density was measured at 620 nm using a PerkinElmer Luminescence Spectrophotometer (Perkin Elmer, Norwalk, CT). EB concentration was calculated using a standard curve and values were normalized to the

tissue weight. Intravascular EB and non-specific effects of injection were accounted for by subtracting the EB extracted after injection of PBS.

Statistical Analysis

Data are expressed as the mean ± SD. Groups were compared with a Student's *t*-test using the statistical software program SigmaStat. $P < 0.05$ was considered significant.

Results

Mast cells express UCP2

We used RT-PCR and immunoblotting to assess expression of UCP2 in murine bone marrow mast cells (BMMCs). The *Ucp2* transcript could be detected by RT-PCR in BMMCs (Fig. 1*A*). Immunoblotting showed that UCP2 protein was expressed in BMMCs, as well as in human leukemic LAD2 mast cells (Fig. 1*B*). No UCP2 was detected in lysate from $Ucp2^{-/-}$ BMMCs, showing the specificity of the antibody (Fig. 1*B*).

Normal development of $Ucp2^{-/-}$ mast cells

BMMCs were obtained by culturing non-adherent bone marrow progenitor cells for 4 weeks in SCF- and IL-3-supplemented media. Bone marrow from both wild-type and $Ucp2^{-/-}$ mice generated highly pure BMMC cultures shown to be morphologically normal with numerous distinguishable granules upon staining with May-Grünwald/Giemsa (Fig. 1*C*). Expression of the mast cell markers c-Kit and FcεRI was assessed by flow cytometry, which showed similar levels of these molecules in wild-type and $Ucp2^{-/-}$ BMMC cultures. (Fig. 1*D*). Expression of FcεRI was also similar following 24 hour incubation with mouse IgE (100 ng/ml; data not shown). Collectively, these results suggest that UCP2 is not necessary for normal BMMC development.

Histamine secretion from $Ucp2^{-/-}$ BMMCs

Following overnight sensitization with DNP-specific IgE (100 ng/ml), BMMCs were stimulated for 20 min with DNP-HSA (10 ng/ml). $Ucp2^{-/-}$ BMMCs released significantly more histamine (1.4-fold) after challenge with 10 ng/ml DNP-HSA (Fig. 2*A*); Levels of basal release were similar in wild-type and $Ucp2^{-/-}$ BMMCs (Fig. 2*A*). We then compared the effect of three different nonimmune triggers in FSMCs: SP (100 μM) and C48/80 (30 μg/ml) as well as the calcium ionophore ionomycin (1 μM), which induces calcium influx. All these non-immune triggers also induced more histamine release from $Ucp2^{-/-}$ mast cells (Fig. 2B), indicating that UCP2 may regulate signaling steps downstream of cytosolic calcium ion influx.

Histamine secretion from UCP-overexpressing human LAD2 mast cells

We next examined the effect of UCP2 on degranulation of human mast cells by transducing LAD2 cells with a lentivirus encoding human UCP2 and green fluorescent protein (GFP) or a lentivirus expressing GFP alone as a control (16). The transduction efficiency was approximately 50% as assessed by flow cytometric analysis of GFP expression; overexpression of UCP2 was confirmed by immunoblot (Fig. 3A). IgE-sensitized UCP2-overexpressing LAD2 cells challenged with anti-IgE (10 ng/ml) had 38% less histamine release compared to control cells (Fig. 3B). Levels of basal histamine release were similar in UCP2-overexpressing and control cells (Fig. 3B). UCP2-overexpressing LAD2 cells stimulated with SP (1 μM) had 23% less histamine release compared to control cells (Fig. 3C). LAD2 cells transduced with the control virus showed similar histamine release to untransduced controls (data not shown). Together, these results suggest that UCP2 down-regulates degranulation in both mouse and human cells regardless of the stimulus used.

UCP2 regulates mast cell histamine content

We next addressed the possibility that UCP2 may affect mast cell histamine content prior to stimulation. Histamine was extracted from the untreated skin of wild-type and *Ucp2*$^{-/-}$ mice and measured by ELISA. Histamine levels were 241 ± 70 nmol/g for wild-type vs. 352 ± 90 nmol/g for *Ucp2*$^{-/-}$ mice (Fig. 4A), a 60% increase over wild-type mice.

Examination of the number and distribution of mast cells in the skin of *Ucp2*$^{-/-}$ mice by May-Grünwald/Giemsa and toluidine blue stains showed no differences from wild-type (Fig. 4B). The skin mast cells had a normal distribution in the superficial dermis with equal numbers in both the *Ucp2*$^{-/-}$ and wild-type skin (Fig. 4C). Given that mast cells are the only cells in the skin to produce histamine and that mast cell density is similar in wild-type and *Ucp2*$^{-/-}$ skin, it suggests that more histamine is produced per mast cell.

We also measured histamine levels in cultured BMMCs and found that wild-type BMMCs contained 0.11 ± 0.029 pg/cell, whereas *Ucp2*$^{-/-}$ BMMCs contained 0.28 ± 0.039 pg/cell, a 155% increase over wild-type cells (Fig. 4D). We next measured the histamine content in LAD2 cells after transduction with either the control or the UCP2-overexpression lentivirus. Transduction with the control lentivirus did not have any effect on LAD2 histamine content. LAD2 cells overexpressing UCP2 had a 27% lower histamine content 5 days after lentiviral transduction (3.63 ± 0.13 pg/cell in control cells vs. 2.60 ± 0.34 pg/cell in UCP2 overexpressing cells; Fig. 4E).

We also measured expression of histidine decarboxylase (HDC), the enzyme responsible for histamine synthesis, to investigate whether this could account for the difference in histamine levels. Quantitative real-time PCR and immunoblot showed that *Ucp2*$^{-/-}$ BMMCs expressed greater levels of HDC mRNA (Fig. 5A) and protein (Fig. 5B). The immunoblot shows both 74 kDa and 54 kDa bands for HDC. The full length HDC (74 kDa) is inactive until it is cleaved to the shorter form (54 kDa). Together, these data indicate that induction of HDC may be responsible for the increased histamine content observed in *Ucp2*$^{-/-}$ mast cells.

UCP2 downregulates superoxide production in many cell types (5)(4). It is also reported that ROS induces the HDC gene (18)(14). We therefore hypothesized that the increased histamine content in *Ucp2*$^{-/-}$ mast cells was due to increased superoxide production. We first showed enhanced ROS production in *Ucp2*$^{-/-}$ BMMCs by measuring fluorescence of cells loaded with dihydroethidium (DHE) using flow cytometry. DHE fluorescence was higher in *Ucp2*$^{-/-}$ BMMCs compared to wild-type BMMCs (Fig. 5C). We examined the effect of mitochondrial superoxide production on histamine content by treating BMMCs with the mitochondrial-targeted superoxide dismutase-mimetic Mn(III) tetrakis (4-benzoic acid) porphyrin (TBAP). Culture of BMMCs for 5 days with TBAP (20–40 μM) reduced histamine content by up to 58% (Fig. 5D). Similar results were found with LAD2 cells (data not shown). Culture of LAD2 cells or BMMCs with TBAP for 5 days did not affect cell viability as shown by Trypan blue staining. These data indicate that mitochondrial superoxide increases histamine content, possibly through induction of HDC.

Ucp2$^{-/-}$ BMMC have higher IL-6 release

Cells were sensitized overnight with anti-DNP IgE (100 ng/ml) and stimulated with DNP-HSA (10 ng/ml) for 24 hours, IL-6 in the supernatant fluid was about 50% higher in the *Ucp2*$^{-/-}$ BMMC than controls (Fig. 6).

Enhanced prostaglandin production and ERK activation in *Ucp2*$^{-/-}$ BMMCs

PGD_2 is a lipid produced primarily by mast cells that contributes to vasodilation, bronchoconstriction and chemotaxis of eosinophils and lymphocytes (19). After stimulation with DNP-HSA (10 ng/ml), *Ucp2*$^{-/-}$ BMMCs produced more PGD_2 (5866±1430 vs. 3274±289 pg/10^6 cells; Fig. 7A). A similar effect was observed with C48/80 (30 μg/ml), (7880±886 vs. 6348±464 pg/10^6 cells; Fig 7B).

ERK is a mitogen-activated protein kinase (MAPK) that controls early-phase prostaglandin production through activation of cytosolic phospholipase A_2 (20) and may also regulate degranulation (21). Its activation is enhanced by ROS (22), raising the possibility that it may link greater ROS production to greater prostaglandin release. We, therefore, measured phospho-ERK levels by immunoblot with the hypothesis that ERK activation would be greater in *Ucp2*$^{-/-}$ BMMCs. Levels of phospho-ERK were higher in *Ucp2*$^{-/-}$ BMMCs following stimulation with both DNP-BSA (Fig. 7B) and C48/80 (Fig. 7D). Levels of total ERK were similar in wild-type and *Ucp2*$^{-/-}$ BMMCs (Fig. 7B, D).

Enhanced vascular permeability in skin of *Ucp2*$^{-/-}$ mice

To assess the effect of UCP2 on mast cell-dependent inflammation *in vivo*, we performed an Evan's blue (EB) extravasation assay following intradermal injection of normal saline or SP (50 pmol) into the dorsal skin. SP mediates stress-induced inflammatory reactions in the skin by activating mast cells (23) and is also upregulated in chronic inflammatory skin diseases such as psoriasis (24,25). SP allows us to measure the effects of direct mast cell activation, since the cells do not need to be sensitized ahead of time. Significantly increased EB extravasation was seen in the skin of *Ucp2*$^{-/-}$ mice following SP injection compared to wild-type mice (Fig. 8A). Similar results were observed in mice passively sensitized by ip injection of anti-DNP IgE and then challenged intradermally with DNP-HSA (Fig. 8B). Capillary permeability caused by mast cell activation is primarily mediated by histamine (24). To rule out the possibility that differences in EB extravasation were due to the response of the capillaries to histamine, we assessed vascular permeability following intradermal injection of histamine (10 μg) into the dorsal skin. No difference in EB extravasation was seen between genotypes (Fig. 8C), indicating that there is a similar response to histamine in both *Ucp2*$^{-/-}$ and wild-type mice. Furthermore, the differences seen in plasma extravasation following either SP or anti-DNP–HSA stimulation cannot be explained by an increased number of mast cells, since we showed that there were no differences in the distribution of skin mast cells in *Ucp2*$^{-/-}$ and wild-type mice (Fig. 4). These data indicate that decreased expression of UCP2 significantly increases mast cell histamine-dependent vascular permeability *in vivo*.

Discussion

Here we show that the mitochondrial protein UCP2 is expressed in both murine and human LAD2 mast cells, and can regulate mast cell activation *in vitro* and *in vivo*. Expression of UCP2 negatively regulated several mast cells functions, including degranulation, histamine production, as well as IL-6 and PGD_2 and release.

The increased skin plasma extravasation seen in *Ucp2*$^{-/-}$ mice can be explained by the increased release of histamine from mast cells since it occurred both after allergic challenge and stimulation with SP, a well-known trigger of mast cells (23). These findings are not due to increased number of mast cells because the number of mast cells in the skin of *Ucp2*$^{-/-}$ mice was similar to that of the wild-type mice. Furthermore, our findings cannot be explained by an augmented response to histamine in *Ucp2*$^{-/-}$ mice, because intradermal

administration of histamine resulted in similar levels of plasma extravasation in both wild-type and *Ucp2*$^{-/-}$ mice.

We found that activation of mast cells with both antigen and FcεRI-independent stimuli (C48/80, SP, ionomycin) resulted in greater histamine release in *Ucp2*$^{-/-}$ cells, whereas overexpression of UCP2 reduced degranulation in LAD2 human mast cells. In agreement with these findings, pharmacologic uncoupling of the mitochondrial proton gradient with FCCP inhibited antigen-induced mast cell degranulation (24). UCP2 was also shown to inhibit exocytosis of insulin granules in β-cells (9), and dopamine-containing vesicles in rat PC12 cells (10).

One possible explanation of our findings is the increased superoxide in the *Ucp2*$^{-/-}$ mast cells. It is known that mast cells produce ROS after stimulation with antigen and non-FcεRI stimuli such as SP and C48/80 (8,26). Inhibition of ROS production by anti-oxidants reduces degranulation and cytokine production (7,27). Povidone-iodine, a superoxide scavenger, inhibited mast cell degranulation *in vitro* (28), and an SOD mimetic decreased mast cell degranulation *in vivo* in a guinea pig model of allergic asthma (29). There are several other endogenous anti-oxidant proteins expressed in mast cells that are reported to affect mast cell activation, including thioredoxin-1 (TRX-1) (7) and heme oxygenase-1 (HO-1) (30). However, UCP2 is the first protein reported to reduce mast cell degranulation that prevents the formation of ROS rather than neutralizing it.

ROS may regulate mast cell degranulation both upstream and downstream of extracellular calcium influx (6,31). Mast cell mitochondria are reported to be involved in the downstream regulation (6). This is in agreement with our results that *Ucp2*$^{-/-}$ mast cells have enhanced degranulation even after calcium ionophore stimulation, where all cells presumably see the same intracellular calcium levels. It is possible that UCP2 affects calcium kinetics since it is involved in mitochondrial calcium uptake (32). Another possibility is that UCP2 decreases ATP levels (33) leading to increased activation of store-operated calcium channels (34).

Increased vascular permeability in the skin of *Ucp2*$^{-/-}$ mice is likely because of increased histamine release due to both increased secretion and increased pre-formed histamine content. The skin of *Ucp2*$^{-/-}$ mice had histamine levels that were 60% higher than controls. Considering the similar number of mast cells, this indicates that there is more histamine stored per cell, a finding we have confirmed in BMMCs. In conjunction with elevated histamine levels, we found that *Ucp2*$^{-/-}$ BMMCs had higher expression of HDC, the enzyme responsible for histamine synthesis. It has been reported that the HDC gene promoter is activated by oxidative stress in AGS gastric cancer cells (18). The higher ROS levels in *Ucp2*$^{-/-}$ mast cells may be responsible for induction of HDC and therefore, increased histamine synthesis. This is consistent with our finding that the SOD-mimetic TBAP decreased histamine levels in both BMMCs and LAD2 cells.

The relation of low *Ucp2* expression to increased mast cell activation was not limited only to histamine since it also permitted higher IL-6 and PGD_2 production and release. Moreover, the greater PGD_2 production in *Ucp2*$^{-/-}$ BMMCs was accompanied by greater ERK phosphorylation. Early prostaglandin synthesis in mast cells is controlled primarily by ERK (20). Oxidative stress is known to induce ERK activation in various cell types, including lymphocytes, possibly through an indirect effect on upstream kinases (22). In addition to prostaglandin release, ERK may regulate degranulation, although there is conflicting evidence for this (20,21).

In addition to our results, other studies have shown that UCP2 plays an important role in other immune responses. UCP2 is also expressed in lymphocytes, dendritic cells, neutrophils and macrophages (35). *Ucp2*$^{-/-}$ mice develop more severe autoimmune encephalomyelitis

(36) and autoimmune diabetes (37). Macrophages from *Ucp2*$^{-/-}$ mice have a greater inflammatory response to lipopolysaccharide (LPS), including increased NF-κB activation and greater cytokine production (11–13). Macrophages overexpressing UCP2 produce less ROS in response to LPS (38) and have decreased transendothelial migration (39). UCP2 deficiency also confers protection to *Toxoplasma gondii* and *Listeria monocytogenes* infection in mice, due to increased inflammatory responses (11,35). Since there is evidence that ROS modulates activation of T and B lymphocytes (40,41), UCP2 may also have important regulatory functions in these cells, although this has not yet been directly explored.

In conclusion, we have identified UCP2 as a novel regulator of mast cell secretion and associated inflammation. Inhibiting UCP2 has been proposed as a method to increase insulin release from β-cells in type 2 diabetes (9). However, inhibition of UCP2 may worsen allergic and inflammatory diseases, making it a less attractive target for this indication. On the other hand, induction or activation of UCP2 may be a new strategy for reducing allergic and inflammatory responses.

Acknowledgments

We thank Sheila Collins for providing the UCP2-deficient breeding pairs, Dr. A.S. Kirshenbaum (NIH, Bethesda, MD) for providing the LAD2 cells and Amgen, Inc. (Thousand Oaks, CA) for their generous gift of hrSCF. We also thank Jessica Christian for help with word processing.

Abbreviations

BMMC	bone marrow mast cell
C48/80	compound 48/80
DNP-HSA	dinitrophenol-human serum albumin
EB	Evan's blue
FSMC	fetal skin mast cell
HDC	histidine decarboxylase
IL-6	interleukin-6
LPS	lipopolysaccharides
SOD	superoxide dismutase
PGD_2	prostaglandin D_2
PMC	peritoneal mast cell
ROS	reactive oxygen species
SP	substance P
TRX	thioredoxin-1
UCP	uncoupling protein

References

1. Galli SJ, Nakae S, Tsai M. Mast cells in the development of adaptive immune responses. Nat Immunol 2005;6:135–142. [PubMed: 15662442]
2. Theoharides TC, Kempuraj D, Tagen M, Conti P, Kalogeromitros D. Differential release of mast cell mediators and the pathogenesis of inflammation. Immunol Rev 2007;217:65–78. [PubMed: 17498052]

3. Theoharides TC, Kalogeromitros D. The critical role of mast cell in allergy and inflammation. Ann NY Acad Sci 2006;1088:78–99. [PubMed: 17192558]
4. Galli SJ, Grimbaldeston M, Tsai M. Immunomodulatory mast cells: negative, as well as positive, regulators of immunity. Nat Rev Immunol 2008;8:478–486. [PubMed: 18483499]
5. Echtay KS. Mitochondrial uncoupling proteins--what is their physiological role? Free Radic Biol Med 2007;43:1351–1371. [PubMed: 17936181]
6. Inoue T, Suzuki Y, Yoshimaru T, Ra C. Reactive oxygen species produced up- or downstream of calcium influx regulate proinflammatory mediator release from mast cells: Role of NADPH oxidase and mitochondria. Biochim Biophys Acta 2008;1783:789–802. [PubMed: 18178162]
7. Swindle EJ, Metcalfe DD. The role of reactive oxygen species and nitric oxide in mast cell-dependent inflammatory processes. Immunol Rev 2007;217:186–205. [PubMed: 17498060]
8. Swindle EJ, Metcalfe DD, Coleman JW. Rodent and human mast cells produce functionally significant intracellular reactive oxygen species but not nitric oxide. J Biol Chem 2004;279:48751–48759. [PubMed: 15361524]
9. Li Y, Maedler K, Shu L, Haataja L. UCP-2 and UCP-3 proteins are differentially regulated in pancreatic beta-cells. PLoS ONE 2008;3:e1397. [PubMed: 18167556]
10. Yamada S, Isojima Y, Yamatodani A, Nagai K. Uncoupling protein 2 influences dopamine secretion in PC12h cells. J Neurochem 2003;87:461–469. [PubMed: 14511123]
11. Arsenijevic D, Onuma H, Pecqueur C, Raimbault S, Manning BS, Miroux B, Couplan E, ves-Guerra MC, Goubern M, Surwit R, Bouillaud F, Richard D, Collins S, Ricquier D. Disruption of the uncoupling protein-2 gene in mice reveals a role in immunity and reactive oxygen species production. Nat Genet 2000;26:435–439. [PubMed: 11101840]
12. Bai Y, Onuma H, Bai X, Medvedev AV, Misukonis M, Weinberg JB, Cao W, Robidoux J, Floering LM, Daniel KW, Collins S. Persistent nuclear factor-kappa B activation in Ucp2−/− mice leads to enhanced nitric oxide and inflammatory cytokine production. J Biol Chem 2005;280:19062–19069. [PubMed: 15757894]
13. Emre Y, Hurtaud C, Nubel T, Criscuolo F, Ricquier D, Cassard-Doulcier AM. Mitochondria contribute to LPS-induced MAPK activation via uncoupling protein UCP2 in macrophages. Biochem J 2007;402:271–278. [PubMed: 17073824]
14. Kirshenbaum AS, Akin C, Wu Y, Rottem M, Goff JP, Beaven MA, Rao VK, Metcalfe DD. Characterization of novel stem cell factor responsive human mast cell lines LAD 1 and 2 established from a patient with mast cell sarcoma/leukemia; activation following aggregation of FcepsilonRI or FcgammaRI. Leuk Res 2003;27:677–682. [PubMed: 12801524]
15. Cao J, Papadopoulou N, Kempuraj D, Boucher WS, Sugimoto K, Cetrulo CL, Theoharides TC. Human mast cells express corticotropin-releasing hormone (CRH) receptors and CRH leads to selective secretion of vascular endothelial growth factor. J Immunol 2005;174:7665–7675. [PubMed: 15944267]
16. Twig G, Elorza A, Molina AJ, Mohamed H, Wikstrom JD, Walzer G, Stiles L, Haigh SE, Katz S, Las G, Alroy J, Wu M, Py BF, Yuan J, Deeney JT, Corkey BE, Shirihai OS. Fission and selective fusion govern mitochondrial segregation and elimination by autophagy. EMBO J 2008;27:433–446. [PubMed: 18200046]
17. Donelan J, Boucher W, Papadopoulou N, Lytinas M, Papaliodis D, Theoharides TC. Corticotropin-releasing hormone induces skin vascular permeability through a neurotensin-dependent process. Proc Natl Acad Sci USA 2006;103:7759–7764. [PubMed: 16682628]
18. Hocker M, Rosenberg I, Xavier R, Henihan RJ, Wiedenmann B, Rosewicz S, Podolsky DK, Wang TC. Oxidative stress activates the human histidine decarboxylase promoter in AGS gastric cancer cells. J Biol Chem 1998;273:23046–23054. [PubMed: 9722530]
19. Pettipher R, Hansel TT, Armer R. Antagonism of the prostaglandin D2 receptors DP1 and CRTH2 as an approach to treat allergic diseases. Nat Rev Drug Discov 2007;6:313–325. [PubMed: 17396136]
20. Kimata M, Inagaki N, Kato T, Miura T, Serizawa I, Nagai H. Roles of mitogen-activated protein kinase pathways for mediator release from human cultured mast cells. Biochem Pharmacol 2000;60:589–594. [PubMed: 10874134]

21. Hanson DA, Ziegler SF. Regulation of ionomycin-mediated granule release from rat basophil leukemia cells. Mol Immunol 2002;38:1329–1335. [PubMed: 12217403]
22. McCubrey JA, Lahair MM, Franklin RA. Reactive oxygen species-induced activation of the MAP kinase signaling pathways. Antioxid Redox Signal 2006;8:1775–1789. [PubMed: 16987031]
23. Suzuki R, Furuno T, McKay DM, Wolvers D, Teshima R, Nakanishi M, Bienenstock J. Direct neurite-mast cell communication *in vitro* occurs via the neuropeptide substance P. J Immunol 1999;163:2410–2415. [PubMed: 10452975]
24. Ohtsu H, Watanabe T. New functions of histamine found in histidine decarboxylase gene knockout mice. Biochem Biophys Res Commun 2003;305:443–447. [PubMed: 12763012]
25. Remröd C, Lonne-Rahm S, Nordliond K. Study of substance P and its receptor neurokinin-1 in psoriasis and their relation to chronic stress and pruritus. Arch Dermatol Res 2007;299:85–91. [PubMed: 17370082]
26. Brooks AC, Whelan CJ, Purcell WM. Reactive oxygen species generation and histamine release by activated mast cells:modulation by nitric oxide synthase inhibition. Br J Pharmacol 1999;128:585–590. [PubMed: 10516636]
27. Suzuki Y, Yoshimaru T, Inoue T, Niide O, Ra C. Role of oxidants in mast cell activation. Chem Immunol Allergy 2005;87:32–42. [PubMed: 16107761]
28. Beukelman CJ, van den Berg AJ, Hoekstra MJ, Uhl R, Reimer K, Mueller S. Anti-inflammatory properties of a liposomal hydrogel with povidone-iodine (Repithel((R))) for wound healing in vitro. Burns 2008;34:845–855. [PubMed: 18378399]
29. Masini E, Bani D, Vannacci A, Pierpaoli S, Mannaioni PF, Comhair SA, Xu W, Muscoli C, Erzurum SC, Salvemini D. Reduction of antigen-induced respiratory abnormalities and airway inflammation in sensitized guinea pigs by a superoxide dismutase mimetic. Free Radic Biol Med 2005;39:520–531. [PubMed: 16043023]
30. Takamiya R, Murakami M, Kajimura M, Goda N, Makino N, Takamiya Y, Yamaguchi T, Ishimura Y, Hozumi N, Suematsu M. Stabilization of mast cells by heme oxygenase-1: an anti-inflammatory role. Am J Physiol Heart Circ Physiol 2002;283:H861–H870. [PubMed: 12181112]
31. Suzuki Y, Yoshimaru T, Matsui T, Inoue T, Niide O, Nunomura S, Ra C. Fc epsilon RI signaling of mast cells activates intracellular production of hydrogen peroxide: role in the regulation of calcium signals. J Immunol 2003;171:6119–6127. [PubMed: 14634127]
32. Trenker M, Malli R, Fertschai I, Levak-Frank S, Graier WF. Uncoupling proteins 2 and 3 are fundamental for mitochondrial Ca2+ uniport. Nat Cell Biol 2007;9:445–452. [PubMed: 17351641]
33. Argiles JM, Busquets S, Lopez-Soriano FJ. The role of uncoupling proteins in pathophysiological states. Biochem Biophys Res Commun 2002;293:1145–1152. [PubMed: 12054495]
34. Rychkov GY, Litjens T, Roberts ML, Barritt GJ. ATP and vasopressin activate a single type of store-operated Ca2+ channel, identified by patch-clamp recording, in rat hepatocytes. Cell Calcium 2005;37:183–191. [PubMed: 15589998]
35. Rousset S, Emre Y, Join-Lambert O, Hurtaud C, Ricquier D, Cassard-Doulcier AM. The uncoupling protein 2 modulates the cytokine balance in innate immunity. Cytokine 2006;35:135–142. [PubMed: 16971137]
36. Vogler S, Pahnke J, Rousset S, Ricquier D, Moch H, Miroux B, Ibrahim SM. Uncoupling protein 2 has protective function during experimental autoimmune encephalomyelitis. Am J Pathol 2006;168:1570–1575. [PubMed: 16651623]
37. Emre Y, Hurtaud C, Karaca M, Nubel T, Zavala F, Ricquier D. Role of uncoupling protein UCP2 in cell-mediated immunity: how macrophage-mediated insulitis is accelerated in a model of autoimmune diabetes. Proc Natl Acad Sci U S A 2007;104:19085–19090. [PubMed: 18006654]
38. Negre-Salvayre A, Hirtz C, Carrera G, Cazenave R, Troly M, Salvayre R, Penicaud L, Casteilla L. A role for uncoupling protein-2 as a regulator of mitochondrial hydrogen peroxide generation. FASEB J 1997;11:809–815. [PubMed: 9271366]
39. Ryu JW, Hong KH, Maeng JH, Kim JB, Ko J, Park JY, Lee KU, Hong MK, Park SW, Kim YH, Han KH. Overexpression of uncoupling protein 2 in THP1 monocytes inhibits beta2 integrin-mediated firm adhesion and transendothelial migration. Arterioscler Thromb Vasc Biol 2004;24:864–870. [PubMed: 15016641]

40. Lee RL, Westendorf J, Gold MR. Differential role of reactive oxygen species in the activation of mitogen-activated protein kinases and Akt by key receptors on B-lymphocytes: CD40, the B cell antigen receptor, and CXCR4. J Cell Commun Signal 2007;1:33–43. [PubMed: 18481208]

41. Williams MS, Kwon J. T cell receptor stimulation, reactive oxygen species, and cell signaling. Free Radic Biol Med 2004;37:1144–1151. [PubMed: 15451054]

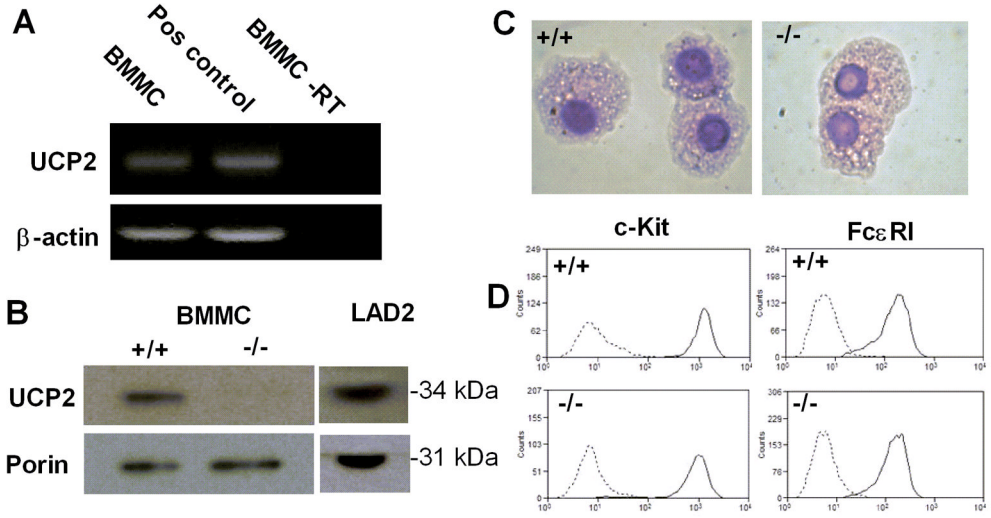

Figure 1. UCP2 is expressed in mouse and human mast cells

(A). RT-PCR for UCP2 and β-actin. Lane 1, cDNA from BMMCs; lane 2, pooled cDNA from mouse brown fat, liver, brain and muscle for positive control; lane 3, BMMC mRNA not reverse transcribed for negative control. Images are representative of three separate experiments with similar results. (B) Immunoblot of lysate from wild-type BMMCs, *Ucp2*$^{-/-}$ BMMCs and LAD2 cells using antibody against UCP2. Immunoblot is representative of three experiments with similar results. (C) Representative May-Grünwald/Giemsa staining of wild-type and *Ucp2*$^{-/-}$ BMMCs. Original magnification, 100x. (D) Flow cytometry of the surface expression of c-Kit and FcεRI in wild-type and *Ucp2*$^{-/-}$ BMMCs. Dotted lines are BMMCs incubated with isotype control antibody. Data is representative of three experiments with similar results.

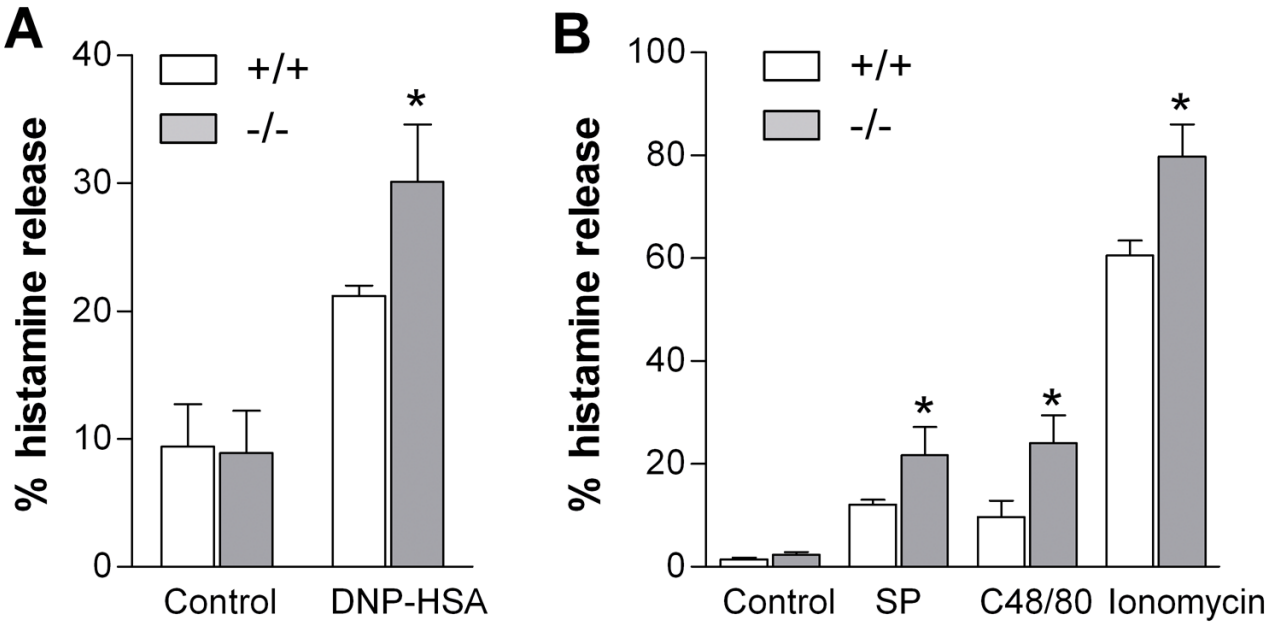

Figure 2. UCP2-deficient mast cells have enhanced degranulation

(A) Wild-type and *Ucp2*$^{-/-}$ BMMCs were sensitized overnight with anti-DNP IgE (100 ng/ml) and challenged for 20 min with DNP-HSA (10 ng/ml). (B) Wild-type and *Ucp2*$^{-/-}$ FSMCs were stimulated for 10 min with SP (100 μM), C48/80 (30 μg/ml), or ionomycin (1 μM), after which histamine was measured in the supernatant and pellet. **P* <0.05 (n=6)

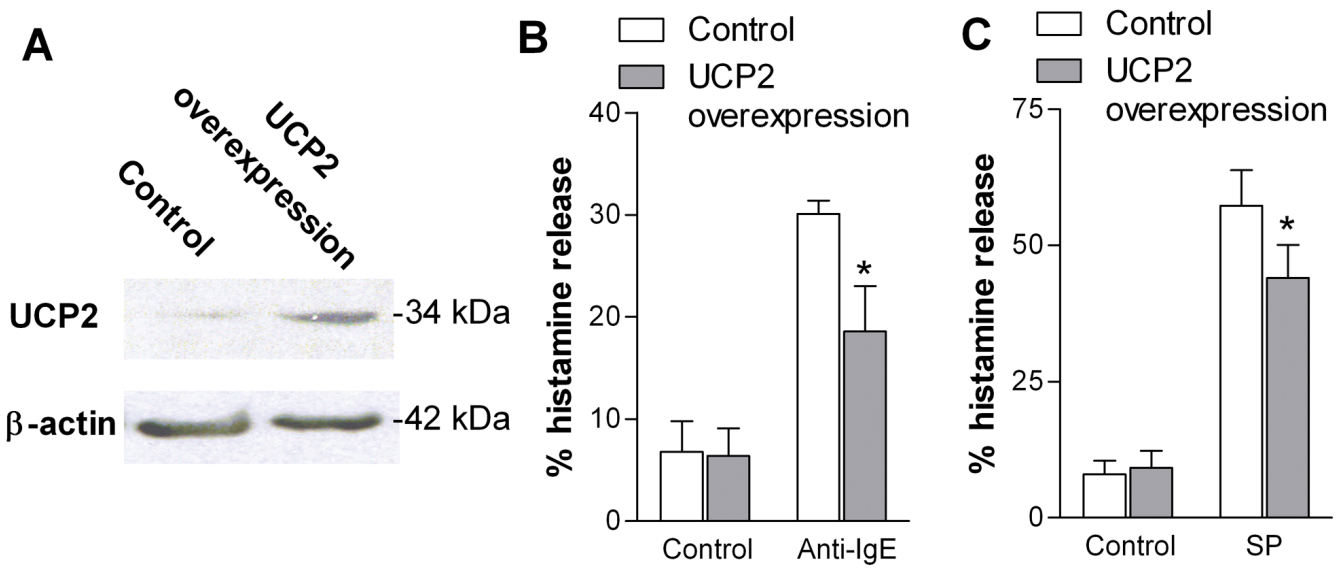

Figure 3. Overexpression of UCP2 in LAD2 cells inhibits histamine release

LAD2 cells were transduced with either a control lentivirus or UCP2 overexpression lentivirus and used for experiments 5 days after transduction. (A) Immunoblot of lysate from transduced LAD2 cells showing UCP2 overexpression. (B) Transduced LAD2 cells were sensitized overnight with human IgE (2 μg/ml) and challenged for 20 min with anti-IgE (10 μg/ml), or (C) stimulated for 10 min with SP (1 μM). **P* <0.05 (*t*-test) vs. cells transduced with control virus. All data are presented as percent histamine release and represent the mean ± SD (n=3).

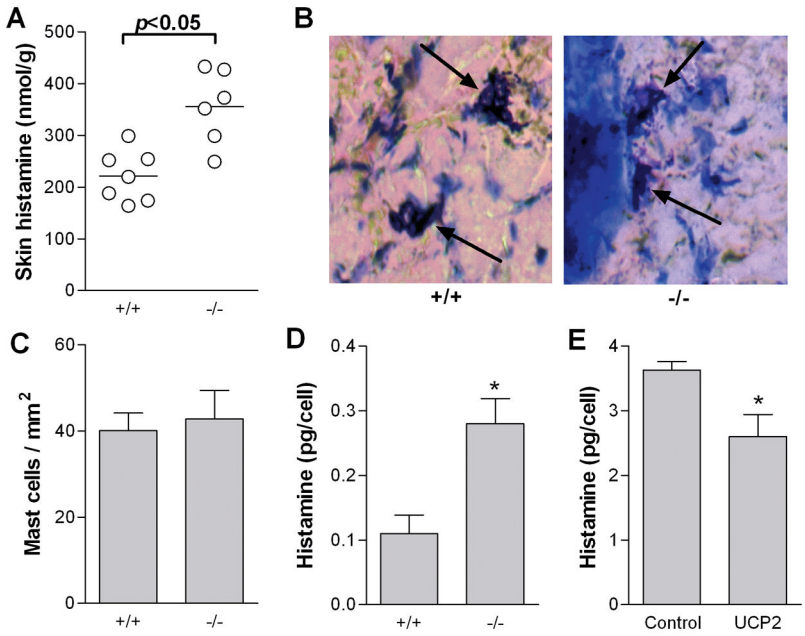

Figure 4. UCP2 decreases mast cell histamine content

(A) Total skin histamine of wild-type and *Ucp2*$^{-/-}$ mice quantified by ELISA. Data are normalized to the tissue weight. **P* < 0.05. Graph represents the mean and individual data of 6–7 mice per genotype. (B) Representative photomicrographs of dorsal skin from wild-type and Ucp2$^{-/-}$ mice stained with toluidine blue. Metachromatic mast cells are also indicated by arrows. (C) Number of mast cells per mm^2 in cross-section of skin. Mast cells were counted in 5 randomly chosen fields from 3 sections per mouse. Data represent the mean ± SD of 5 mice per genotype. *P* > 0.05. (C) Total histamine content of wild-type and *Ucp2*$^{-/-}$ BMMCs was measured spectrophotometrically and normalized to cell number. **P* < 0.05 vs. wild-type (*t*-test). Data is the mean ± SD of three experiments. (D) Total histamine content of LAD2 cells 5 days after transduction with a control lentivirus or UCP2 overexpression lentivirus. **P* < 0.05 vs. control cells. Data is the mean ± SD (n=3).

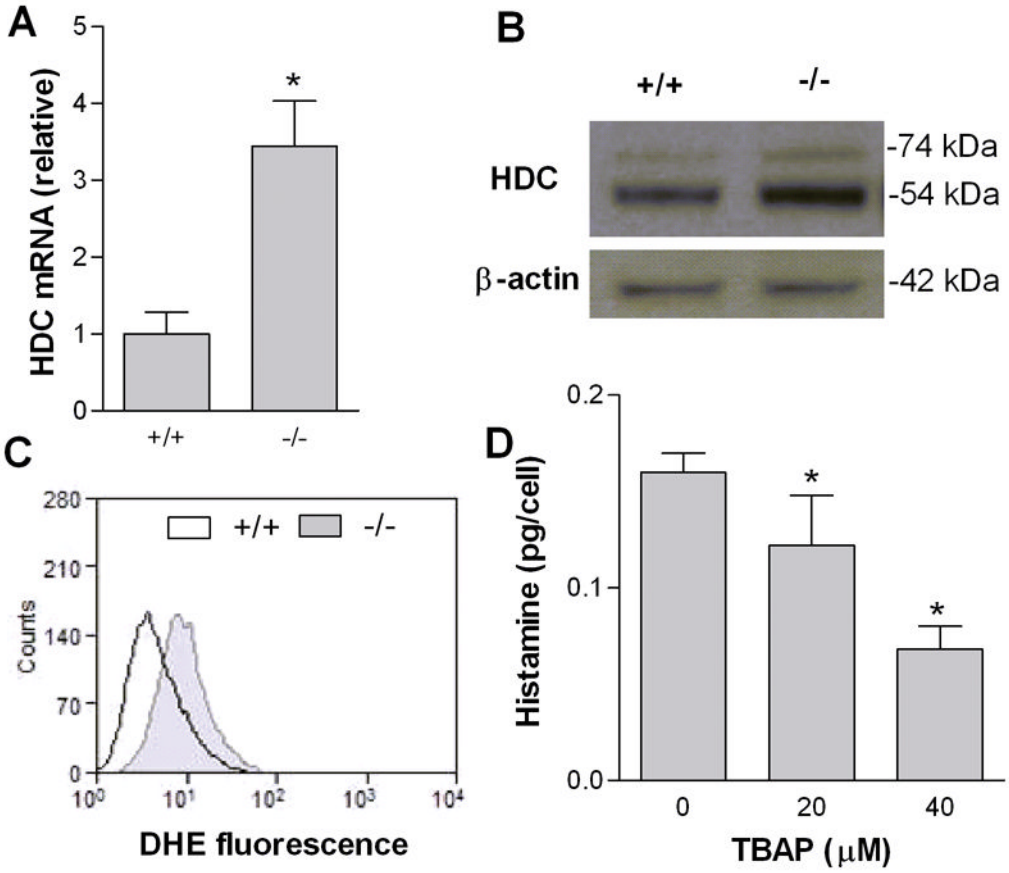

Figure 5. UCP2 decreases mast cell histidine decarboxylase expression

(A) Real-time quantitative PCR of *histidine decarboxylase* mRNA transcripts from wild-type and *Ucp2*$^{-/-}$ BMMCs normalized to 18s rRNA. **P* < 0.05. Data are the mean ± SD of three experiments. (B) Immunoblot of lysate from wild-type and *Ucp2*$^{-/-}$ BMMCs with anti-HDC antibody. Immunoblot is representative of three independent experiments with similar results. (C) Superoxide production of wild-type and *Ucp2*$^{-/-}$ BMMCs measured by dihydroethidium using flow cytometry. Histogram is representative of three experiments with similar results. (D) Total histamine content of BMMCs after 5 day treatment with TBAP (20–40 μM). **P* < 0.05. Data are the mean ± SD (n=3).

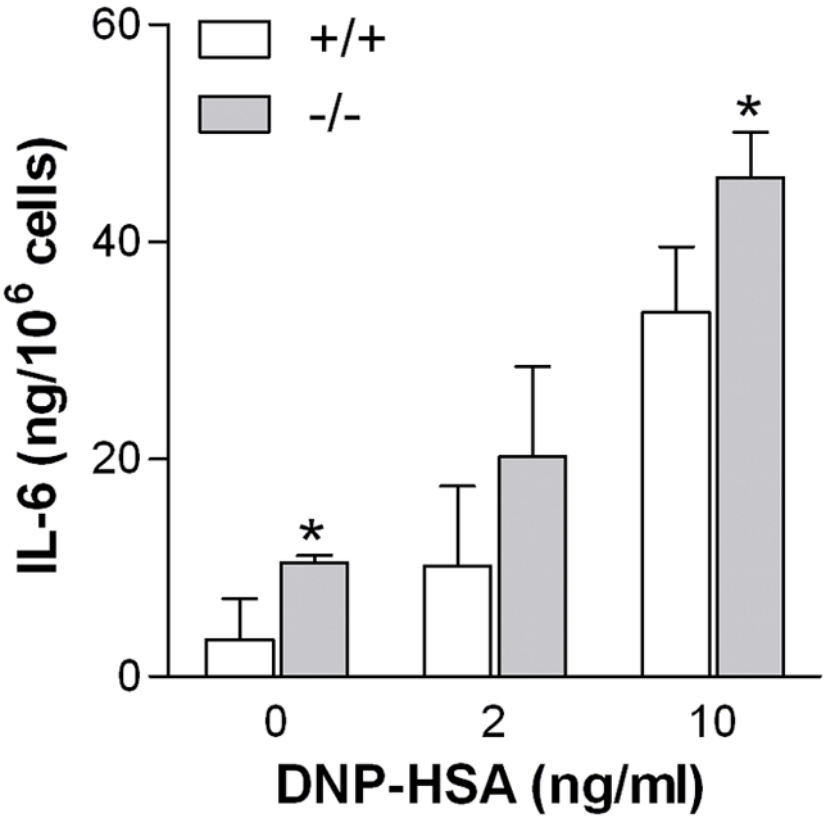

Figure 6. ***Ucp2*$^{-/-}$ BMMC have augmented IL-6 release**

Cells were sensitized overnight with anti-DNP IgE (100 ng/ml) and stimulated with DNP-HSA (10 mg/ml) in complete medium. After 24 hours, IL-6 in the supernatant fluid was measured by ELISA (n=3, *p<0.05).

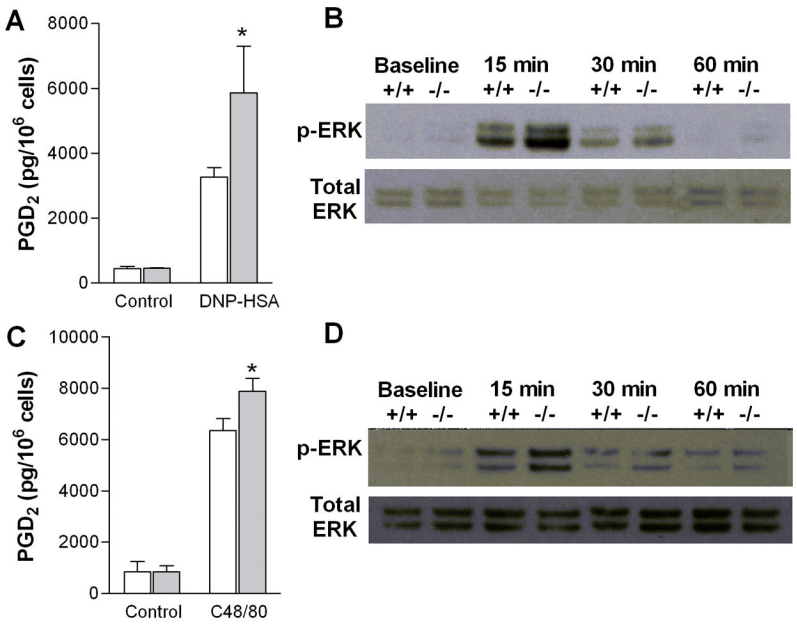

Figure 7. *Ucp2*$^{-/-}$ BMMCs have augmented PGD_2 release and ERK activation

(A,C) PGD_2 release from wild-type and *Ucp2*$^{-/-}$ BMMCs. Cells were either (A) sensitized overnight with anti-DNP IgE (100 ng/ml) and stimulated with DNP-HSA (10 ng/ml). or (C) stimulated with C48/80 (30 μg/ml); after 30 min, supernatant PGD_2 was measured by ELISA. **P* <0.05 vs. wild-type. All data represent the mean ± SD of three experiments. (B,D) ERK phosphorylation in wild-type and *Ucp2*$^{-/-}$ BMMCs. Cells were treated for the indicated times as follows; (*B*) sensitized overnight with anti-DNP IgE (100 ng/ml) and then stimulated with DNP-HSA (10 ng/ml), or (D) stimulation by C48/80 (30 μg/ml), Phospho-ERK and total ERK were determined by immunoblot. Immunoblots are representative of three experiments with similar results.

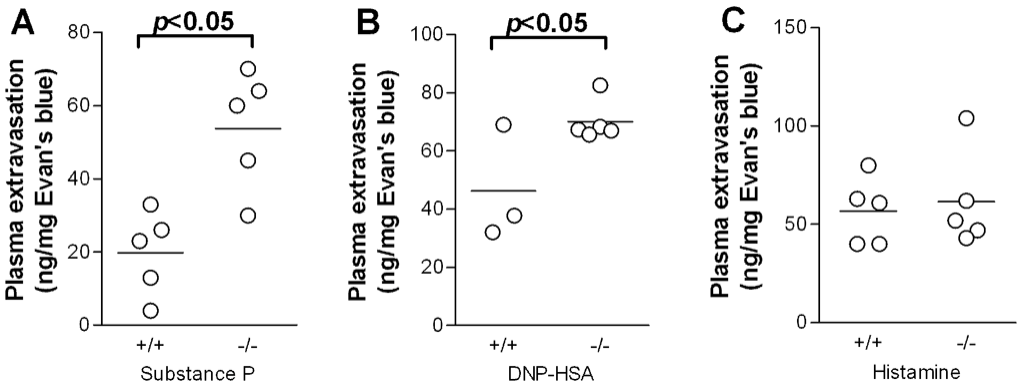

Figure 8. Enhanced vascular permeability in *Ucp2*$^{-/-}$ mouse skin

(A) Evans blue extravasation following intradermal injection of either normal saline and SP (50 pmol) for 10 min. (B) Evan's blue extravasation following passive sensitization with IgE and local skin challenge with DNP-HSA for 10 min. (C) Evans blue extravasation after intradermal challenge with histamine (10 μg) for 10 min. Evans blue was extracted from the injection sites in N,N-dimethylformamide overnight, quantified by absorbance at 620 nm and normalized to tissue weight. All results represent net extravasation after subtraction of extravasation from control saline injections. *P<0.05. Graphs represent the mean and individual values of each mouse.